METALS AND MATERIALS International, Vol. 7, No. 1 (2001), pp. 61~65

Double Loop Electrochemical Potentiokinetic Reactivation Test of Nickel-Base Alloy 600 Surface-Melted by a CO_2 Laser Beam

Y.S. Lim, H.P. Kim, J.S. Kim, and H.S. Kwon*

Steam Generator Materials Project, Korea Atomic Energy Research Institute
P.O. Box 105, Yusong-ku, Taejon 305-600, Korea
*Department of Materials Science and Engineering
Korea Advanced Institute of Science and Technology
373-1 Kusung-dong, Yusong-ku, Taejon 305-701, Korea

Ni-base Alloy 600 has been widely used as a steam generator (S/G) tubing material in nuclear power plants because of its good mechanical and corrosion properties at high temperatures. However, degradations of S/G tubes due to intergranular attack (IGA) and intergranular stress corrosion cracking (IGSCC) during normal operation have been frequently reported. In particular, Alloy 600 can be very susceptible to IGA/IGSCC in some sulfur-bearing environments by sensitization. In this paper, the beneficial effects of laser surface melting (LSM) on intergranular corrosion of the sensitized Alloy 600 is presented from the results of the double loop electrochemical potentiokinetic reactivation (DL-EPR) test. The DL-EPR test was performed in de-aerated 0.01 M H_2SO_4+20 ppm KSCN at a scan rate of 0.5 mV/sec at room temperature. The degree of sensitization (DOS) of the sensitized Alloy 600 measured from the DL-EPR test was considerably reduced by LSM. The sensitized Alloy 600 after LSM also exhibited a relatively low DOS, compared with that of the sensitized but not laser treated Alloy 600. From the microscopic observation, it was found that the microstructural changes brought about by the LSM process, especially changes in the precipitation behavior of grain boundary Cr-rich carbides, caused the improvement of resistance to intergranular corrosion of the laser treated Alloy 600. The resistance to IGSCC of the laser treated Alloy 600 in sulfur-bearing environments was also discussed from the results of measured DOS and microstructural examination.

Keywords : Alloy 600, laser surface melting, sensitization, DL-EPR test, intergranular corrosion

1. INTRODUCTION

It is now well recognized that Ni-base Alloy 600 is susceptible to inter-granular attack/intergranular stress corrosion cracking (IGA/IGSCC) under pressurized water reactor operating conditions [1]. In particular, the precipitation of Cr carbides and the resultant creation of Cr depleted zones in the vicinity of the grain boundaries (commonly called sensitization) is known to play an important role in determining the alloys susceptibility to IGA/IGSCC [2]. Once sensitized, Alloy 600 can suffer a vital intergranular fracture in sulfur-bearing environments such as sodium thiosulfate ($Na_2S_2O_3$), and sodium tetrathionate ($Na_2S_4O_6$) solutions even at low temperatures [3].

Laser surface melting (LSM) is one of the laser application techniques which can improve the surface properties of materials such as corrosion and wear. LSM can be applied to repair the tubes degraded by IGA/IGSCC during the normal operation of nuclear power plants, since the laser beam can easily be directed to the failed parts through a beam transmission system such as an optical fiber. From previous studies, it was demonstrated that LSM improved the resistance to IGA/IGSCC of the sensitized Alloy 600 in sulfur-bearing environments [4], mainly due to the metallurgical changes induced by the laser treatment [5]. During failure by IGSCC, a crack starts at the free surface and propagates through a connected pathway of the susceptible grain boundaries. Therefore, the corrosion resistant surface formed by LSM can provide an effective barrier between the corrosion environment and the underlying sensitized alloy.

The double loop electrochemical potentiokinetic reactivation (DL-EPR) test, originally proposed by Umemura *et al.* [6], was found to be fast, quantitative, and reproducible in measuring the degree of sensitization (DOS) of alloys. The

This article based on a presentation made in the symposium “The 4th International Conference on Fracture and Strength of Solid”, held at POSTECH, Pohang, Korea, August 16-18 under the auspices of Far East and Ocean Fracture Society (FEOFS), *et al*.

Table 1. Chemical composition of the specimen used (wt.%)

Ni	Cr	Fe	C	N	S	Si	Al	Ti	Nb	Mg
Bal.	15.9	7.6	0.04	0.04	0.002	0.15	0.12	0.21	tr.	0.008

DL-EPR method has also been used for providing an indication of sulfur compound attack susceptibility to IGSCC by measuring DOS in the alloys.

The present work was aimed at investigating the effects of LSM on the intergranular corrosion of the sensitized Alloy 600 by DL-EPR test. The measured DOS under the given DL-EPR testing condition was analyzed in terms of the microstructural changes caused by the LSM process. Finally, the resistance to IGSCC of the laser treated Alloy 600 in sulfur-bearing environments was evaluated from the experimental results.

2. EXPERIMENTAL PROCEDURES

2.1. Specimen preparation

Mill annealed Alloy 600 plates 1.6 mm thick were used in this study, the alloy composition of which is shown in Table 1. The specimens were sealed in a quartz tube, solution annealed at 1050°C for 30 minutes, and then water quenched (hereafter referred to as SA Alloy 600 for short). Some of the SA Alloy 600 were subsequently sensitized at 600°C for 24 hours and then followed by furnace cooling (hereafter SA+SEN Alloy 600).

A continuous CO_2 laser beam was used; details of the LSM procedure are described elsewhere [5]. Some of the LSM specimens (hereafter LSM Alloy 600) were also subsequently sensitized under the same conditions as for the SA+SEN Alloy 600 (hereafter LSM+SEN Alloy 600). The specimens for scanning electron microscopy (SEM) observation were made by etching the polished samples with a solution of 2% HCl and 98% methanol at 6 V for about 3-5 seconds.

2.2. DL-EPR test

Cu-wire was spot-welded to one side of each specimen, mounted in epoxy resin, and ground to 2000 grade silicon carbide. To avoid crevice corrosion, the specimen-mount interface was carefully coated with a thin film of silicone sealant. Approximately 1 cm^2 of the surface was exposed to the test solution. All solutions were prepared from double-distilled water and the chemicals of analytical-grade reagents. The test solution chosen for the evaluation of DOS in Alloy 600 was 0.01 M H_2SO_4 with an addition of 20 ppm KSCN. The test solutions were de-aerated by purging with purified N_2 gas, before and during each DL-EPR test.

The DL-EPR test was performed using a three-electrode cell system consisting of a saturated calomel electrode (SCE) as a reference, a platinum (Pt) electrode as a counter, and a specimen as a working electrode. The sample was kept immersed in the test solution for 0.5-1 hour at open-circuit potential. After obtaining the stable corrosion potential (E_{corr}), it was raised in the anodic direction, from the value of E_{corr} to a potential in the passive range, at a scan rate of 0.5 mV/sec. After attaining the pre-determined potential (600 mV_{SCE}), it was followed by a reactivation scan back to E_{corr}. All the potentials are referred to a saturated calomel electrode (SCE). All the tests were performed at a room temperature of 25-27°C. The DL-EPR test in different solutions was repeated at least twice for each specimen to ensure reproducibility.

3. RESULTS

3.1. Results from DL-EPR test

Before a DL-EPR test, an immersion test of C-ring specimens was primarily conducted to confirm the effects of the sensitization heat treatment on the fracture behavior of Alloy 600 in 0.1 M $Na_2S_4O_6$ solution. After 18 hours of immersion, cracking was found to start on the outer-diameter side, and the maximum-length crack propagated into approximately 80% of the thickness of the C-ring after 86 hours of immersion. The fracture surfaces after C-ring test revealed a fully intergranular type, as shown in Fig. 1(a). From the above results, it can be concluded that the sensitization treatment at 600°C for 24 hours was suitable for exhibiting a high susceptibility to IGSCC for Alloy 600 in the sulfur-bearing corrosive environments.

Fig. 1(b) shows a DL-EPR curve typically obtained from the SA+SEN Alloy 600 under the present DL-EPR testing conditions. DOS is defined, in Fig. 1(b), as the percent ratio of the maximum current density in the reactivation loop (I_r) to that in the anodic loop (I_a), i.e., $I_r/I_a \times 100$. It is evident from Fig. 1(c) that the measured DOS values from the LSM Alloy 600 and LSM+SEN Alloy 600 were considerably reduced by the laser treatment. The average DOS value of the LSM Alloy 600 was measured as 3.42, which was considerably lower than 16.5 of the SA+SEN Alloy 600. The average DOS value of the LSM+SEN Alloy 600 was measured as 8.71, which was still lower than that from the SA+SEN Alloy 600. From the above results, it can be concluded that the LSM Alloy 600 and the LSM+SEN Alloy 600 are more resistant to intergranular corrosion than the SA+SEN Alloy 600 in the given corrosive environment.

3.2. Microstructural examination

Fig. 2(a) shows a typical distribution of intergranular Cr-rich carbides in the SA+SEN Alloy 600. By sensitization

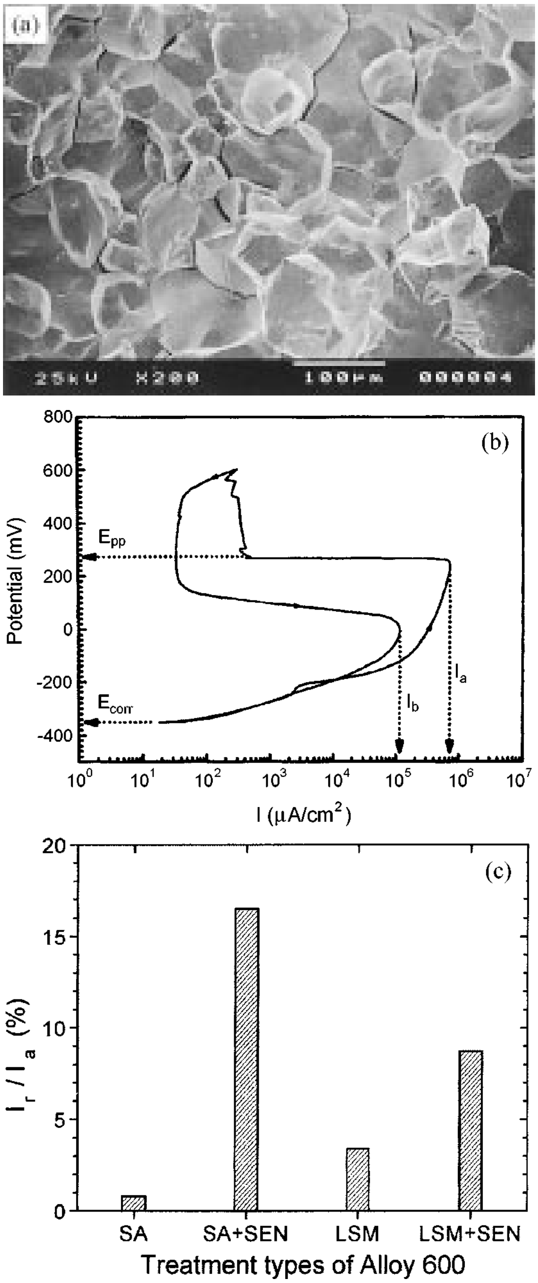

Fig. 1. (a) Fracture surface of the SA+SEN Alloy 600 after C-ring test, (b) a typical DL-EPR curve, and (c) DOS measured from the differently treated Alloy 600. (b) and (c) were obtained in 0.01 M H_2SO_4 +20 ppm KSCN solution at a scan rate of 0.5 mV/sec at room temperature.

treatment, nearly continuous Cr-rich carbides were precipitated on most of the grain boundaries, excluding the special boundaries such as coherent twin boundaries and low-angle grain boundaries, as shown in the figure. The high DOS values of the SA+SEN Alloy 600 should, therefore, reflect the distribution morphology of Cr-rich carbides and the severe Cr depletion along the grain boundaries in the alloy. The typical microstructures of the LSM Alloy 600 and the LSM +SEN Alloy 600 are shown in Figs. 2(b) and (c), respectively.

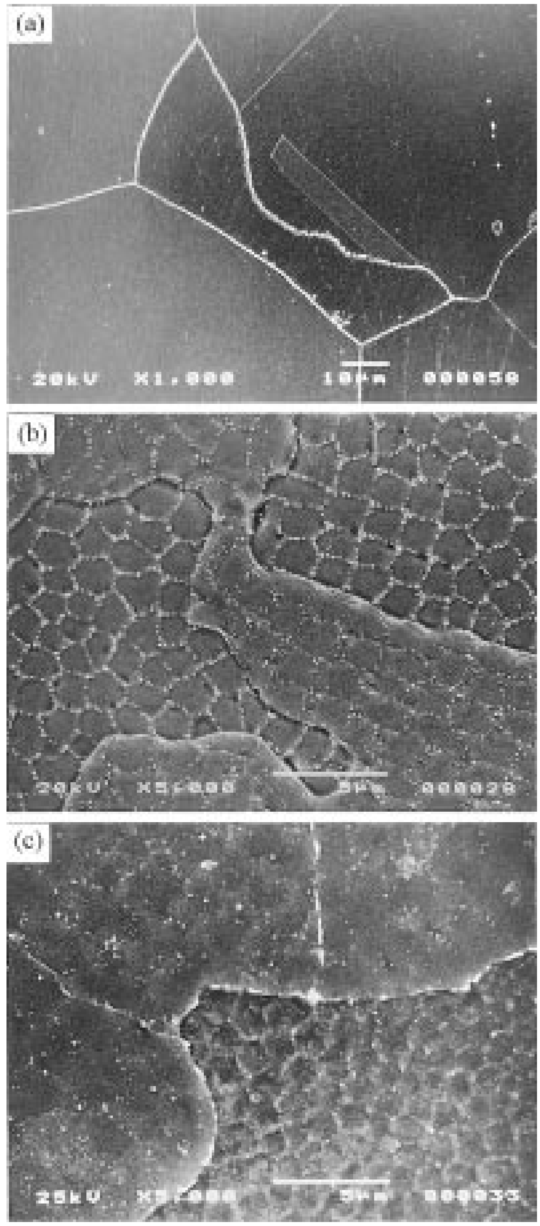

Fig. 2. Typical microstructures of (a) the SA+SEN Alloy 600, (b) the LSM Alloy 600, and (c) the LSM+SEN Alloy 600, etched in a solution of 2% HCl and 98% methanol.

Fig. 2(b) shows the particles formed in the laser melted zone (LMZ) during the LSM process. No Cr-rich carbides are seen on the grain boundaries in Fig. 2(b). This result originates from the fact that pre-existing Cr-rich carbides of the sensitized Alloy 600 were completely melted/dissolved due to the high energy density of a laser beam. Moreover, Cr-rich carbides were not re-precipitated due to the high cooling rate during the LSM process [5]. Therefore, low DOS of the LSM Alloy 600 is caused by the de-sensitization (or, disappearance of the Cr depletion zones) due to the LSM process. The tiny particles along the cell boundaries, identified as TiN and MgS, are formed by dissolution and subsequent re-precipitation of the pre-existing coarse TiN and MgS inclusions in the commercial Alloy 600 during the LSM process [7].

The second phases in the LSM+SEN Alloy 600 are shown in Fig. 2(c). There were no noticeable changes in the tiny particles of TiN and MgS caused by the sensitization treatment. However, some Cr-rich carbides are seen on some grain boundaries in Fig. 2(c). These were identified as Cr-rich $M_{23}C_6$ and Cr_7C_3 [8], the same found in the case of the SA+SEN Alloy 600 [5]. The average size of the Cr-rich carbides precipitated on the grain boundaries in the LSM+SEN Alloy 600 was much smaller than that in the SA+SEN Alloy 600. Moreover, they were sparsely distributed on grain boundaries, and were found only on some high angle grain boundaries. The degree of Cr depletion on the grain boundaries was, therefore, not severe. The minimum Cr concentration on the grain boundaries was measured as 12 wt% [8], which was considerably higher than the 7.3 wt% of the SA+SEN Alloy 600 [5]. Therefore, it can be concluded that the laser treatment suppressed the precipitation of grain boundary Cr-rich carbides in Alloy 600, and this led to the low DOS value of the LSM+SEN Alloy 600.

3.3. Surface morphologies after DL-EPR test

The grain boundary attack in the SA+SEN Alloy 600 after the DL-EPR test is shown in Fig. 3. The grain boundary attack was clearly revealed by the addition of 20 ppm KSCN, without any intergranular and intragranular pitting (Fig. 3(a)). This demonstrates that the DL-EPR testing conditions employed in the present experiment were suitable for measuring the degree of sensitization of the fully sensitized Alloy 600, i.e., grain boundary attack occurred without any noticeable general corrosion or pitting corrosion in the matrix.

The grain boundary attacks in the LSM Alloy 600 and the LSM+SEN Alloy 600 after the DL-EPR tests are shown in Figs. 3(b) and (c), respectively. The LSM Alloy 600 did not experience any grain boundary attacks, as shown in Fig. 3(b). The white contrast along the cell boundaries in Fig. 3(b) resulted from the different dissolution rates of the elements. Chromium was more enriched along the cell boundaries due to the micro-segregation formed during the laser treatment [5]. The regions around the cell boundaries were, therefore, more corrosion resistant due to the enriched Cr content than those inside the cells in acidic solutions. Fig. 3(c) shows the grain boundary attack in the LSM+SEN Alloy 600. As shown in the Figure, only some grain boundaries were discretely attacked, and the attacked morphology denotes exactly the distribution of grain boundary Cr-rich carbides (Fig. 2(c)).

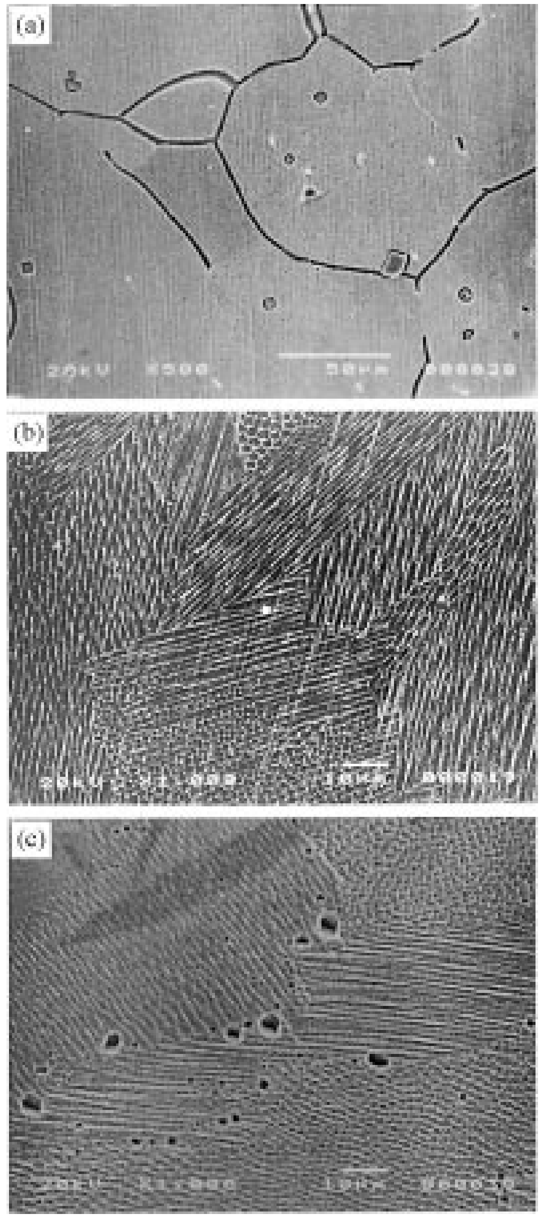

Fig. 3. SEM micrographs showing the surface morphologies after DL-EPT test for (a) the SA+SEN Alloy 600, (b) the LSM Alloy 600, and (c) the LSM+SEN Alloy 600, in 0.01 M H_2SO_4+20 ppm KSCN solution at a scan rate of 0.5 mV/sec at room temperature.

4. DISCUSSION

Ahn *et al.* [9] suggested the optimized DL-EPR testing conditions be performed in de-aerated 0.01 M H_2SO_4+20 ppm KSCN solution at a scan rate of 0.5 mV/sec at room temperature to predict the susceptibility to IGSCC in $Na_2S_4O_6$ solutions by the measured DOS. However, the optimized conditions can vary from test to test due to different heat treatment procedures resulting in different extents of grain boundary Cr depletion in the alloys. In the present study, the best results were obtained with the addition of 20 ppm KSCN, i.e., clean grain boundary attacks and the suppression of general and pitting corrosion.

The average DOS value was considerably reduced, and grain boundary attack was not observed in the LSM Alloy 600 (Figs. 1(c) and 3(b)). From the microstructural examination, it was demonstrated that the microstructural changes of the grain boundaries in the sensitized Alloy 600 brought about by the LSM process resulted in the improvement of the resistance to intergranular corrosion of the alloy. Suh *et al.* [4] found that the fracture mode of the sensitized Alloy 600 was changed by LSM, i.e., from a brittle intergranular fracture of the SA+SEN Alloy 600 to a typical ductile transgranular failure of the LSM Alloy 600. Moreover, the stress corrosion cracks propagating from the free surface into the center of the sensitized specimen were arrested by the laser-melted track, making further propagation into the laser treated region impossible [4].

No continuous grain boundary attack was observed in the LSM+SEN Alloy 600 with sufficiently reduced DOS value (Figs. 1(c) and 3(c)). Was *et al.* [10] found, from Heuy and Streicher tests, that severe IGA occurred when the measured Cr concentration on the grain boundary was below 9 wt% with a nearly continuous distribution of grain boundary Cr-rich carbides. Therefore, the LSM+SEN Alloy 600 should have a high resistance to IGA in acidic environments. Kai *et al.* [2] showed that the critical Cr concentration to prevent the IGSCC failure was around 8 wt% from the constant load test with the applied stress of 390 MPa, pH of 3, and $Na_2S_2O_3$ concentration of 0.001 M to 0.1 M at room temperature. Therefore, it can also be expected that the LSM+SEN Alloy 600 will have a high resistance to IGA/IGSCC in sulfur-bearing environments as well.

5. CONCLUSIONS

(1) The sensitization treatment of Alloy 600 at 600°C for 24 hours induced a severe brittle intergranular fracture in neutral 0.1 M $Na_2S_4O_6$ solution, due to the precipitation of nearly continuous grain boundary Cr-rich carbides and the severe Cr depletion on the grain boundaries. The present DL-EPR testing conditions revealed a high DOS value in the sensitized Alloy 600 with suppression of other types of corrosion such as general and pitting corrosion.

2. LSM improved the resistance to IGA/IGSCC of the sensitized Alloy 600 by sufficiently reducing the average DOS value. The average DOS value of the LSM+SEN Alloy 600 was also much lower, compared with that of the SA+SEN Alloy 600. From these results, it can be expected that the LSM Alloy 600 and the LSM+SEN Alloy 600 will have a high resistance to IGA/IGSCC in acidic and sulfur-bearing environments. Consequently, the LSM technique was shown to be an attractive method for repairing the failed S/G tubes in nuclear power plants.

ACKNOWLEDGMENT

This work has been carried out as a part of the Steam Generator Materials Project under the Nuclear R & D Program by M.O.S.T. in Korea.

REFERENCES

1. T. U. Marston and R. L. Jones, *Proc. 5th Int. Symp. on Environmental Degradation of Materials in Nuclear Power Systems-Water Reactors* (eds., D. Cubicciotti, E. P. Simonen and R. E. Gold), p. 3, ANS, La Grange Park, Illinois (1991).
2. J. J. Kai, C. H. Tsai, T. A. Huang and M. N. Liu, *Metall. Trans. A* **20**, 1077 (1989).
3. R. C. Newman, R. Roberge and R. Bandy, *Corrosion* **39**, 386 (1983).
4. J. H. Suh, J. K. Shin, Y. S. Lim, I. H. Kuk and J. S. Kim, *Mater. Sci. Eng. A* **254**, 67 (1998).
5. Y. S. Lim, J. H. Suh, I. H. Kuk and J. S. Kim, *Metall. Mater. Trans. A* **28**, 1223 (1997).
6. F. Umemura, M. Akashi and T. Kawamoto, *Corros. Eng*. **29**, 163 (1980).
7. Y. S. Lim, J. S. Kim and H. S. Kwon, *Metall. Mater. Trans. A* (2001) to be published.
8. Y. S. Lim, J. S. Kim and H. S. Kwon, *Mater. Sci. Eng. A* **279**, 192 (2000).
9. G. S. Was, H. H. Tischner and R. M. Latanision, *Metall. Trans. A* **12**, 1397 (1981).
10. M. K. Ahn, H. S. Kwon and J. H. Lee, *Corrosion* **51**, 441 (1995).